3D printed Shape Memory Alloy Wire Embedded Actuator

Md Najmul Islam*
Electrical Engineering
The University of Texas at Tyler
Tyler, TX, USA
mislam6@patriots.uttyler.edu

Mario Barron Gonzalez*
Mechanical Engineering Program
University of Houston – Clear Lake
Houston, TX, USA
BarronGonzal@UHCL.edu

Shawana Tabassum
Electrical Engineering
The University of Texas at Tyler
Tyler, TX, USA
stabassum@uttyler.edu

Kazi Md Masum Billah Mechanical Engineering Program University of Houston – Clear Lake Houston, TX, USA billah@uhcl.edu

Abstract— Thermoplastic Polyurethane is best known for its elastic and flexible qualities. 3D printing of polyurethanes is well-evolved research for various applications including soft robotics, actuators, and origami structures. In this research, we developed a polyurethanes-based composite actuator that uses commercially available nickel-titanium alloy - Nitinol shape memory alloy. The Nitinol wire is embedded within a 3Dprinted thermoplastic polyurethane substrate. 3D printing "Pause and Go" approach is used to add the pause during the printing of the specimen and insert the SMA wire. After embedding the wire, printing is continued to complete the fabrication of the specimen with embedded wire. Several design configurations were fabricated in the exploratory research to understand the impact of the geometry on the actuation. Through the experimental characterization, we observed the actuation due to external thermal and electrical stimulation. The embedded SMA regained the treated shape which ultimately demonstrated the actuation. This research explores the low-cost manufacturing of soft robotics elements which can be used in many real-life applications in medical, aerospace, and domestic appliances.

Keywords—3D printing, Additive Manufacturing, Actuator, Nitinol, Wire Embedding.

I. INTRODUCTION

Shape memory alloy (SMA) is a material capable of transitioning to a pre-trained shape when subjected to temperature variations. The ability to exhibit this property is known as the shape memory effect (SME). The intrinsic SME property of the SMA wire is a result of phase transformation due to the temperature change. Diffusion-less austenite to martensite (A

M) crystallographic transformation leads to the shape changes of SMA wire [1]. The reversible phase transformation of martensite to austenite $(M \rightarrow A)$ can be done by changing the temperature and this process is repeatable to a great extent. SMAs are an emerging class of materials due to their unique shape and phase transformation properties. Compared to other engineering materials, SMAs are a relatively new class of materials and have gained significant attention for the soft robotics actuation application [2]. In actuation-based application, SMA-based parts provide several advantages compared to the traditional high reversible strains (up to 6%) and shape recovery, high damping capacity, large reversible change of mechanical and physical characteristics, and the ability to generate high recovery stresses when they are prevented from recovering their shape [3].

Although SMA wires are extensively utilized in composite actuator structures, the manufacturing process chain has remained notably outdated. In recent years, SMA wires have been used in 3D-printed structures for actuator applications. As an example, one-shot additive manufacturing which is known as the 3D printing approach was used to develop an SMA wire-embedded composite actuator [4]. This process demonstrated the manufacturing of SMA based actuator for self-sensing. The manufacturing process for the actuator involved some manual steps, particularly in embedding the wire within the plastic substrate, necessitating a preformed channel to facilitate wire insertion. This particular manufacturing process yields poor adhesion and bonding between the substrate and wire, therefore impacting the actuation under external stimulation. In another work [5], SMA wire was embedded within the 3D-printed substrate using a custom-made wire embedding tool. While this technology was promising to automate the process, the thermal embedding process of the wire yielded defects at the interface of the wire and substrate material. The thermal embedding process melted the substrate to immerse the wire and create fusion bonding. However, defects introduced at the interface during this process could potentially affect the actuation performance.

In this research, we investigated the fabrication of an SMA-based actuator composite part that is made of thermoplastic polyurethane (TPU) and net thermoplastic material such as Acrylonitrile Styrene Acrylate (ASA). In our manufacturing process, we used a non-polar solvent to embed the SMA wire within the 3D-printed substrate. In addition, we investigated several design configurations to co-relate with the actuation capability.

II. MATERIALS AND METHOD

A. 3D printing of actuator

In this research, we used Nitinol SMA wire from Kellogg's Research Lab (New Boston, NH, USA). The wire diameter was approximately 0.50 mm or 24 AWG. To fabricate the Nitinol wire embedded parts, we used a desktop scale Raise3D E2 3D printer (Irvine, CA, USA). Our overall research goal was to demonstrate the manufacturing of shape memory alloys wearing an embedded soft actuator. Thermoplastic polyurethane (TPU) filament feedstock was used for its flexible property. In addition, acrylonitrile styrene acrylate (ASA) filament was used as the interfacial material

between the nitinol wire and TPU. Both filaments have a diameter of 1.75 mm. A representative processing chain of the specimen fabrication is shown in Figure 1.

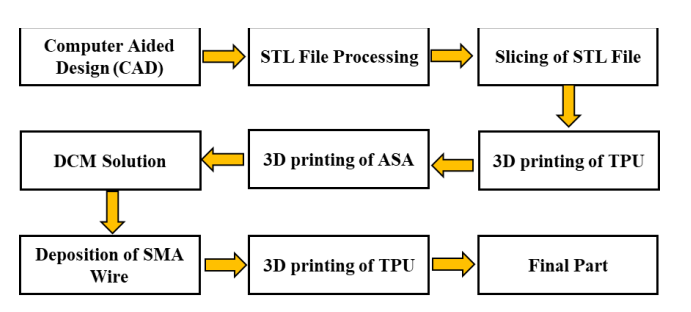


Figure 1: Flow chart showing the steps from the initial part design to manufacturing.

In our initial investigation, we used TPU as the outer layer material of the specimen due to its elastic properties. TPU can withstand the frequent actuation of the SMA wire within. A thin layer of ASA was inserted between two TPU layers to act as an adhesive for the wire. After the completion of ASA printing, a pause, previously integrated into the G-code, was initiated to commence the immersion process of the SMA wire. The printing bed temperature was adjusted to 100°C, with the TPU extrusion temperature set to 250°C and ASA to 255°C. Since the printer is enclosed, the high temperature remains contained within the printer, rather than being exposed to the surrounding ambient temperature, which might cause the part to warp. We used a non-polar solvent such as Dichloromethane (DCM) on top of the thin ASA layer to slightly soften it. DCM solvents are commonly used in solution casting 3D printing to prepare the casted feedstock materials [6]. The DCM solvent allowed the nitinol wire to be manually inserted and submerged, so that, it remained flush with the ASA. Once the wire is properly seated, the rest of the TPU is printed on top, resulting in the final specimen. Figure 2 below shows a representative specimen of the initial design.

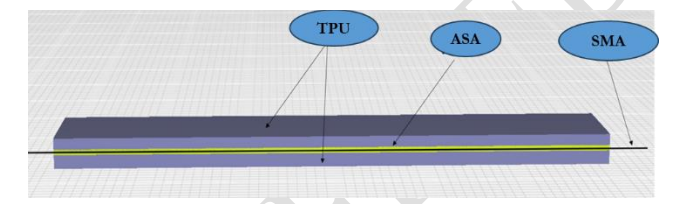


Figure 2: Design for the 3D printed actuator with embedded SMA wire.

Although our initial design of the SMA wire embedded actuator proved effective, our objective was to reduce both the surface area and the amount of TPU used in the 3D printed specimen, thereby minimizing the area through which the wire would need to move. This resulted in a second and more favorable design shown in Figure 3. The new design has relatively less material within the part, thus shortened the print time for the part by approximately 35%.

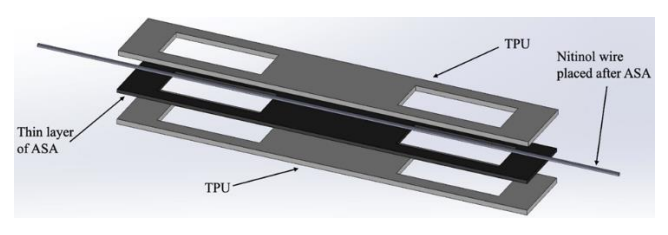


Figure 3: Updated design for the 3D printed actuator with embedded SMA wire.

B. Training of SMA wire

The nitinol SMA wire was pre-trained by the manufacturer. We reshaped the wire by training at different temperatures for our design. To retrain the wire, a wooden block with nails inserted into the desired curved shape of the wire was used. As per the manufacturer's recommendation, a temperature above 200 °C was required to retrain the wire. The manufacturer's guidance suggests that heating the wire until it glows red, and then quickly quenching it in water will set the new shape. Figure 4 shows the schematic of the wooden block used to train the wire. We used a propane-based hand torch for heating and training the wire.

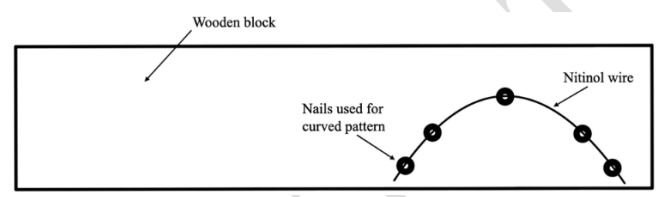


Figure 4: Schematic of wooden block with nails set in the desired shape.

III. EXPERIMENTAL SETUP

The SMA wire embedded specimen was tested to observe the actuation capability under the electrical loadings. Ohmic heating was performed on the embedded SMA wire using a DC power supply. The experiment utilized an Agilent Triple output DC power supply, the E3631A model, capable of delivering a maximum voltage of ±25 V with a maximum current of 1A, or alternatively, 0-6V with 5A current. For this experiment, the 0-6 V section of the power supply was employed due to its ability to meet the high current requirements for heating the nitinol wire. measurements were validated using an HP 34401A multimeter to ensure measurement accuracy, while the temperature of the nitinol wire was monitored using a Tektronix DMM916 multimeter equipped with a K-type thermocouple probe. Figure 5 shows the setup used to test the specimen where a 3D-printed structure was used to hold the SMA specimen and measure the actuation angle. Figure 5 also shows the specimen being connected to the power supply by using two alligator clips. The red and white ends of the alligator clips represent the positive and the negative connectors, respectively. Actuation of the SMA wire requires heating the wire to more than 40°C to produce the ohmic heating effect on the SMA wire.

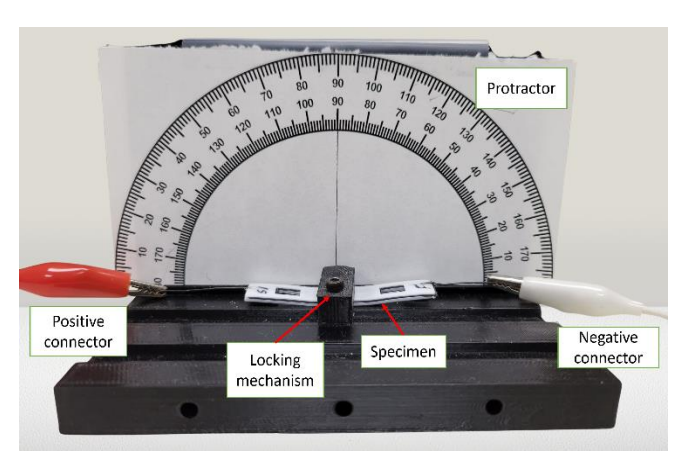


Figure 5: The SMA specimen is locked in the middle and connected to the power supply with two power connectors.

IV. RESULTS AND DISCUSSION

In this experiment, various parameters, including voltage, current, actuation angle, temperature, and resistance of the nitinol wire, were analyzed to gain a comprehensive understanding of the performance metrics of the SMA wire. The wire was excited with a voltage from 0V to 2.3V. The voltage was increased in 0.1V increments, with a consistent duration of 10 minutes for each interval. Measurements of current, temperature, and bending angle were taken three times during each 10-minute interval and later averaged to get more stable and reliable results. All measurements were conducted at an ambient temperature of 24.2°C.

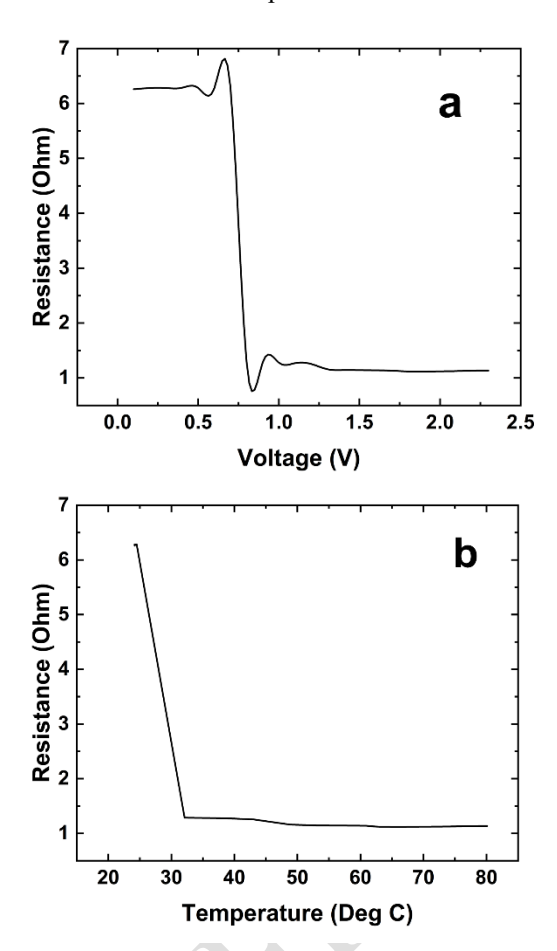


Figure 6: Resistance of the SMA wire as a function of a) applied voltage and b) measured temperature along the wire.

The resistance of the nitinol wire varied in response to changes in applied voltage, as shown in Figure 6a. The resistance of the nitinol wire was determined using Ohm's law, given the applied voltage and measured current. Initially, between 0.1V and 0.7V, the resistance remained relatively stable at around 6.2 Ω but sharply decreased to 1.29 Ω at 0.8V when the temperature of the wire reached 32.1°C, as shown in Figure 6b.

At 2.3V the wire temperature reached 80.1°C, which was the maximum operation temperature of the specimen. The temperature vs voltage plot, as shown in Figure 7a, indicates a noticeable increase in temperature beginning at 0.8V, before that it remained consistent at the ambient temperature of 24.2°C. Therefore, it can be inferred that, for this particular nitinol wire, the threshold voltage for heating the wire is 0.8V. The nitinol wire demonstrated an almost linear relationship between temperature rise (i.e., the difference

between the wire and ambient temperature values) and power consumption, as illustrated in Figure 7b. The power loss to heat the nitinol wire was calculated from the measured voltage and current.

Actuation in the SMA specimen was observed at 1.2V in Figure 8a; prior to that point, no noticeable change in the bending angle occurred, although the wire temperature started to rise at 0.8V. Subsequently, actuation increased progressively with rising voltage levels. No angular change or actuation was detected until the wire temperature reached 40°C, as shown in Figure 8b; nevertheless, past this threshold, a nearly linear actuation pattern became apparent.

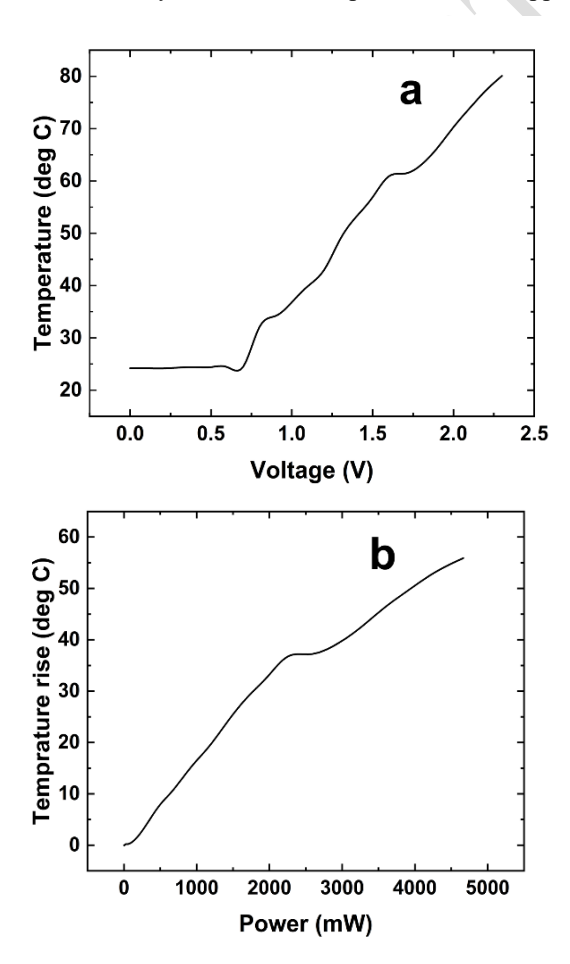
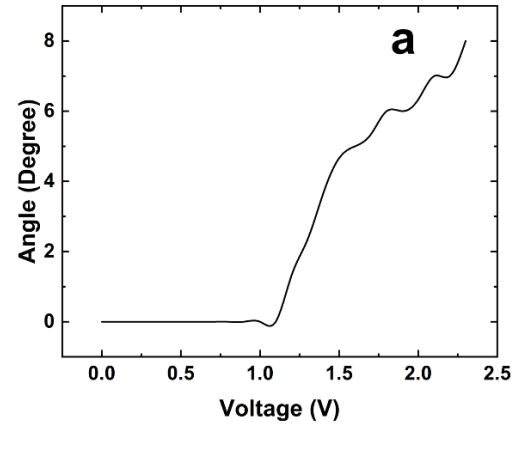


Figure 7: Temperature of the SMA wire as a function of a) applied voltage and b) input power loss.

These experiments demonstrate that when the SMA specimen was excited at 0.8V, coinciding with a reduction in its resistance to 1.29 Ω , there was an initial rise in the wire temperature, but without any noticeable actuation. However, actuation commenced when the applied voltage reached 1.2V and the wire temperature attained 40°C, continuing until the wire reached the maximum allowable temperature of the specimen. Beyond this temperature, the 3D-printed parts in the specimen started to melt.

Furthermore, we tested two identically prepared samples to assess their reliability. Both samples exhibited very similar resistance characteristics, as depicted in Figure 9a. However, some variations were observed in the actuation angle (see Figure 9b), possibly attributable to fluctuations in temperature during the wire reshaping process. Besides, one

of the measurement limitations encountered was the manual angle measurement, providing a resolution of only 1°. To



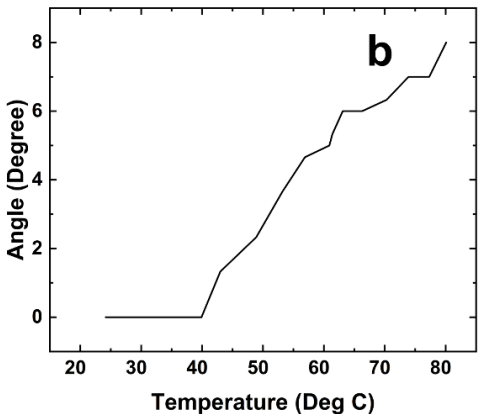
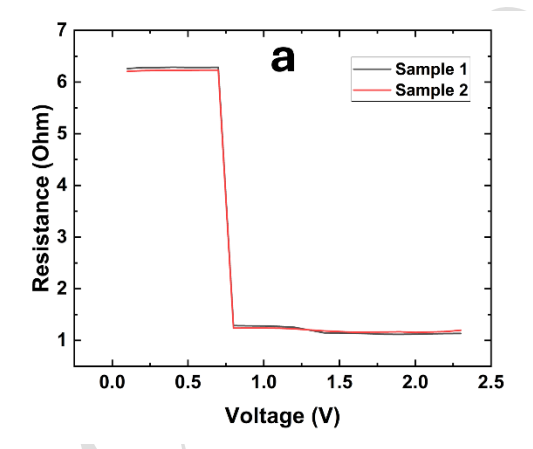


Figure 8: Actuation angles across various a) applied voltage and b) measured temperature levels.



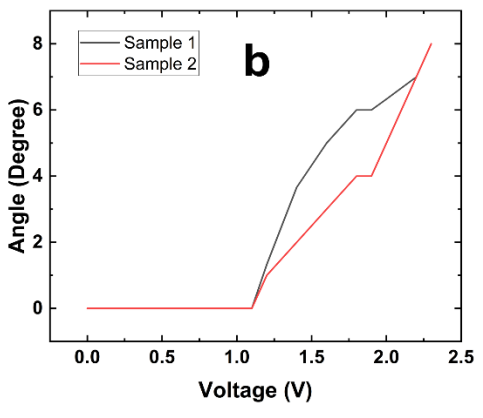


Figure 9: Comparison between two samples based on the a) Resistance and b) Actuation angle as a function of the voltage applied across the wire.

address this constraint, further work will involve implementing an image processing-based algorithm aimed at enhancing measurement accuracy [7].

V. CONCLUSION

In this research, we demonstrated the manufacturing of an SMA wire-based actuating composite structure with a reduced processing chain. The use of a non-polar solvent DCM to immerse the wire yielded defect-free specimens. Electrical characterization such as resistance heating test for the actuation showed the actuation capabilities of the fabricated specimens. While some specimens showed repeatability in the actuation, some specimens did not show repeated actuation due to improper wire training. In this exploratory research, we used the flame torch for training the wire which can be done in a more controlled way to train the wire. In the future, we envision training the wire at a more precise and specific temperature. To control the actuation in a fixed temperature window, wire training should be performed in a similar temperature range.

ACKNOWLEDGMENT

Part of this work is based upon work supported by the National Science Foundation under Grant No: 2301925. Dr. Billah is grateful to the Pathway to STEM Career Grant at UHCL for providing research opportunities to undergraduate students and supporting various experimental setups. He is also grateful to the UHCL Mechanical Engineering program for allowing access to the research and teaching facilities and testing equipment used throughout this endeavor.

Another part of this work is supported by the National Science Foundation under Grant No: 2138701 and The United States Department of Agriculture under Grant No: 58-6030-3-005.

*Authors contributing equally to this work.

REFERENCES

- [1] J. Bhaskar, A. Kumar Sharma, B. Bhattacharya, and S. Adhikari, "A review on shape memory alloy reinforced polymer composite materials and structures," *Smart Mater. Struct.*, vol. 29, no. 7, p. 073001, Jul. 2020, doi: 10.1088/1361-665X/ab8836.
- [2] Lee, JH., Chung, Y.S. & Rodrigue, H. Long Shape Memory Alloy Tendon-based Soft Robotic Actuators and Implementation as a Soft Gripper. Sci Rep 9, 11251 (2019). https://doi.org/10.1038/s41598-019-47794-1
- [3] G. Song, B. Kelly, and B. N. Agrawal, "Active position control of a shape memory alloy wire actuated composite beam," Smart Mater.

- Struct., vol. 9, no. 5, p. 711, Oct. 2000, doi: 10.1088/0964-1726/9/5/316.
- [4] "One-shot additive manufacturing of robotic finger with embedded sensing and actuation | The International Journal of Advanced Manufacturing Technology." Accessed: Mar. 13, 2024.
- [5] A. Fernandez, "Development of actuators using material extrusion additive manufacturing with embedded shape memory alloy wire" [Master's Thesis, The University of Texas at El Paso, 2019], Digital Commons at UTEP.
- [6] Sato, S., Gondo, D., Wada, T., Kanehashi, S. and Nagai, K. (2013), Effects of various liquid organic solvents on solvent-induced crystallization of amorphous poly(lactic acid) film. J. Appl. Polym. Sci., 129: 1607-1617. https://doi.org/10.1002/app.38833.
- [7] Peilin Li, Mustafa Ucgul, Sang-Heon Lee, Chris Saunders, "A new approach for the automatic measurement of the angle of repose of granular materials with maximal least square using digital image processing", Computers and Electronics in Agriculture, Volume 172, 2020, 105356, ISSN 0168-1699, https://doi.org/10.1016/j.compag.2020.105356.